

## **ELECTROMAGNETIC SUSCEPTIBILITY OF AN ELECTROMAGNETIC BAND-GAP FILTER STRUCTURE**

**Y. H. Lee and S. Y. Huang**

School of Electrical and Electronic Engineering  
Nanyang Technological University  
50 Nanyang Avenue, Singapore 639798, Singapore

**Abstract**—In a dual-plane compact electromagnetic band-gap (C-EBG) microstrip structure, patches are etched periodically in the ground plane to prohibit the propagation of electromagnetic waves in certain frequency bands so as to provide filtering functionality. However, the existence of the etched patches in the ground plane becomes a natural concern for the reason that these structures might be more prone to electromagnetic interference from nearby radiating components as compare to a microstrip filter with a perfect ground plane. In this paper, an investigation into the electromagnetic susceptibility of a C-EBG filter structure is presented. This study examines the effects of the interference source on the performance of a C-EBG structure in terms of the relative frequency, power level, position, and polarization. From the study, useful guidelines are drawn for the applications of EBG microstrip structures in an environment rich in electromagnetic interference.

### **1. INTRODUCTION**

Electromagnetic band-gap (EBG) structure has been a term widely accepted nowadays to name the artificial periodic structures that prohibit the propagation of electromagnetic waves at microwave or millimeter wave frequencies. Base on the dimension of EBG unit cells, they could be categorized into three-dimensional (3-D) and planar EBG structures. Due to the unique stopband and slow-wave effect, planar EBG structures have been widely applied in designs of planar filters for the optimization of performance and miniaturization of the circuit [1, 2].

---

Corresponding author: S. Y. Huang (HUAN0104@ntu.edu.sg).

A 1-D EBG microstrip reflector [3] is a simple EBG microstrip structure with two-dimensional EBG units arranged in a single plane. It exhibits a prominent stopband in a certain frequency band. However, it is a compromise between good filtering performance and compact physical size. In [4], a dual-plane EBG configuration was proposed where EBG cells are arranged in both the MLIN and the GND plane in a particular manner to obtain good filtering functionality with a small number of EBG cells (small circuit area). With the application of tapering techniques, the proposed dual-plane compact EBG (C-EBG) structure shows advantages of excellent stopband and passband performance, small circuit area, easy fabrication, and compatibility with monolithic circuits.

In most planar EBG structures including the aforementioned C-EBG structure, periodic patches are etched in the GND plane. The etched patches enhance the inductive effect thus the filtering functionality. However, it becomes a natural concern that these etched holes make the structure sensitive to the environment in which it is intended to operate.

Some studies on the electromagnetic compatibility (EMC) of an EBG structure have been conducted. It was reported that the  $S$ -parameters of a 2-D EBG microstrip filter structure are influenced by a uniform shielding plate in close proximity to the structure [5]. In [6], the susceptibility of an EBG microstrip structure with etched periodic defected ground structure (DGS) unit cells in the GND plane was further investigated. The influence of a metallic enclosure on the  $S$ -parameters of a shielded EBG microstrip structure and that of a finite ground plane on the performance of an unshielded EBG structure are both studied. The influence on the stopband of an unshielded structure is significant when the width of the ground plane is small with respect to the size of the etched patch. The influence of an upper wall or a lower wall of the metallic enclosure is also considered. The paper goes on to suggest the use of a finite ground plane or a metallic enclosure to shield EBG structures from interference. This makes the circuit bulky and complex. Little is known of the EMC of an EBG structure to microstrip lines and other circuit components when they are incorporated into a system without shielding. Some results are presented on the electromagnetic susceptibility (EMS) of an EBG microstrip structure to interference introduced by a nearby radiating circuit component such as an antenna, or through the coupling from a neighboring microstrip line in [7] and [8], respectively.

In this paper, a systematic study on the EMS of the dual-plane C-EBG filter structure in [4] in an EM environment rich in interference is presented. Interferences that are caused either by a radiating

component or by a coplanar MLIN are included in this investigation. Experimental results are presented and analyzed. When the device under test (DUT) is subjected to a radiating interference source, the effects of frequency and power variations, as well as the relative position and polarization of the interference source to the DUT are investigated. When the DUT is subjected to an interference caused by a coplanar MLIN, two types of effects are examined. One is the EM effect of the coplanar MLIN on the  $S$ -parameters of the DUT when the coplanar MLIN is a passive component. The other is the EM influence caused by the coplanar MLIN when a signal is transmitted through both the coplanar MLIN and the DUT. Through this study, some useful guidelines can be obtained when applying a C-EBG structure into an EM rich environment.

In Section 2, a brief introduction to the DUT is given. This is followed by the investigation into the susceptibility of the DUT to the interference caused by either a radiating interference source or a coplanar MLIN (Sections 3 and 4). In Sections 3 and 4, the corresponding experimental setup, results and analysis are presented.

## 2. DEVICE UNDER TEST

Figure 1 shows the 3-D view of the dual-plane C-EBG structure under investigation (the DUT) [4]. It has circular patches etched in the GND plane at a period of  $a_1$  and rectangular patches inserted in the MLIN at a period of  $a_2$  forming a dual planar EBG configuration,  $a_1 = a_2 = a$ . With the unique dual planar configuration, the C-

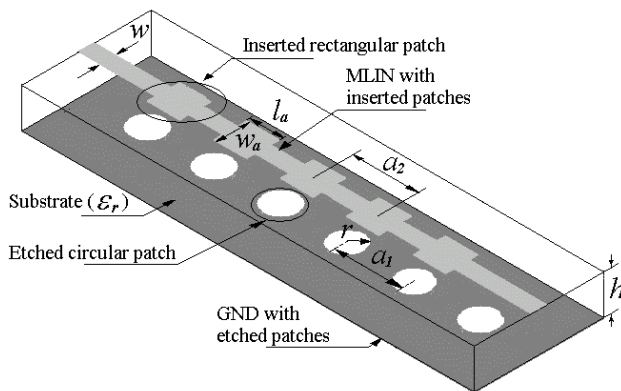


**Figure 1.** 3-D view of the dual-plane compact EBG (C-EBG) microstrip filter structure under EMC test.

EBG structure demonstrates the advantages of high selectivity, and high attenuation and large bandwidth of the stopband. This high performance filter structure is very useful since it is easy to fabricate and it is compatible with MMICs. However, little is known of its EMC performance and its functionality when the structure is working in an environment with EM interference.

The DUT is fabricated using Taconic ( $\epsilon_r = 2.43$ ,  $h = 30$  mils) as the substrate of the C-EBG structure. The center frequency of the stopband of the EBG structure,  $f_0$ , is designed to be 10 GHz. Thus, the periods of the structure,  $a_1$  and  $a_2$ , are determined to be 10.35 mm according to the Bragg reflection condition [3]. The width of the MLIN,  $w$ , is set to be 2.29 mm corresponding to a characteristic impedance of  $50 \Omega$ . The width and the length of the inserted patch in the MLIN,  $w_a$  and  $l_a$ , are both set to be 5 mm in order to achieve an optimal filling factor of 0.25 [9]. The radius of the etched circuits is 2.59 mm with the filling factor,  $r_1/a_1 = 0.25$  which is consistent with that of the inserted patches. The structure is simulated using the method-of-moments (MoM)-based software,  $IE3D^{TM}$ . It is fabricated and tested. Fig. 2 shows its simulated and measured  $S$ -parameters. As can be seen in Fig. 2, the measured results are in good agreement with the simulated results. The ripples in the passband can be suppressed by applying tapering techniques [4]. With the tapering techniques, a tapered C-EBG structure is able to achieve an insertion loss (ripple level) of less than 1 dB in the passband [4]. In order to simplify the study on EMS, the DUT is a non-tapered C-EBG structure.

In practical applications, it is common for an EBG structure to

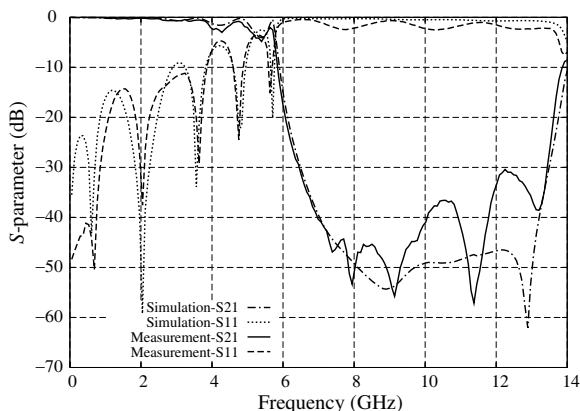


**Figure 2.** The simulated ( $IE3D^{TM}$ ) and measured  $S$ -parameters of the dual-plane C-EBG filter structure [4].

work in an environment rich in EM radiation or with a transmission line operating in close proximity to the structure. Therefore, the susceptibility of the DUT in the above two possible electromagnetic environments is important information when integrating the high performance EBG filter structure into circuit designs. The EM susceptibilities of the C-EBG structure to these two interference source (radiation and coplanar MLIN) are investigated in the following sections.

### 3. INTERFERENCE CAUSED BY RADIATING SOURCE

#### 3.1. Experimental Setup

In this part of the study, the DUT is subjected to a radiating interference source to examine its EMS. A signal is transmitted through the filter structure while a series of patch antennas are used to generate the radiating interference. Fig. 3(a) shows the cross-sectional view of the DUT with a patch antenna in close proximity. As can be seen in Fig. 3(a), an interference source is placed  $d$  away from the plane under test (PUT) with an angle of incidence at  $\theta$  (with respect to the PUT). The DUT is tested within both near-field (Fresnel region) and the far-field (Fraunhofer region) of the interference source. The inner boundary,  $R_1$ , and outer boundary,  $R_2$ , of the radiating near-field region can be approximated using (1) and (2), respectively [10].

$$R_1 = 0.62\sqrt{D^3/\lambda} \tag{1}$$

$$R_2 = 2D^2/\lambda \tag{2}$$

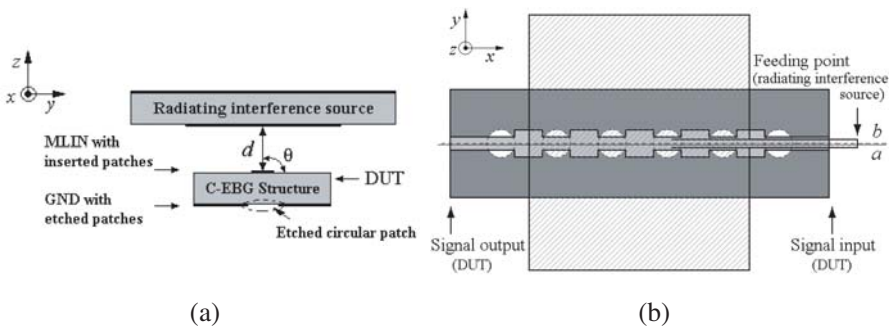


**Figure 3.** (a) Cross sectional view and (b) top view of the experimental setup for the EMS test.

where  $D$  is the maximum dimension of the antenna. It equals the diagonal length of the patch antennas used in the test. For testing in the near-field region and far-field region,  $d$  is set such that  $R_2 > d > R_1$  and  $d > R_2$ , respectively.  $\theta$  defines the angle of incidence of the radiating with respect to the PUT of the C-EBG filter structure.  $\theta$  is positive when the MLIN plane is exposed to the interference and it has a negative value when the GND plane is exposed to the interference. In Fig. 3(a),  $\theta$  equals  $-90^\circ$ .

Figure 3(b) shows the top view of the experimental setup. As shown in Fig. 3(b), the angle between the line of symmetry of the C-EBG filter,  $a$ , and that of the patch antenna,  $b$ , is denoted by  $\phi$ . It defines the relative polarization between the radiating interference source and the signal transmission in the DUT. When  $\phi = 0^\circ$ , as shown in Fig. 3(b), the  $E$ -field of the antenna is in the same polarization as that of the signal transmitted through the C-EBG filter.

Figure 4 shows the block diagram of the EMC test on the DUT. A frequency modulated (FM) sinusoidal signal is generated using signal generator 1 and transmitted through the DUT at a carrier frequency,  $f_c$ . This FM signal is observed and demodulated at the output of structure using a spectrum analyzer. Another signal is generated using signal generator 2 and radiated using a patch antenna at a frequency of  $f_i$ , generating a radiating interference. The DUT is subjected to this radiating interference therein the noise peak-to-peak (P-P) voltage of the demodulated signal at the output of the DUT is recorded.

A relative noise P-P voltage of the demodulated signal is used as a parameter to evaluate the EMS characteristics of the DUT. It is denoted using  $r_n$  and it is defined as a ratio between the measured noise P-P voltage of the demodulated signal when the DUT is exposed to an interference and that of the signal when there is no interference

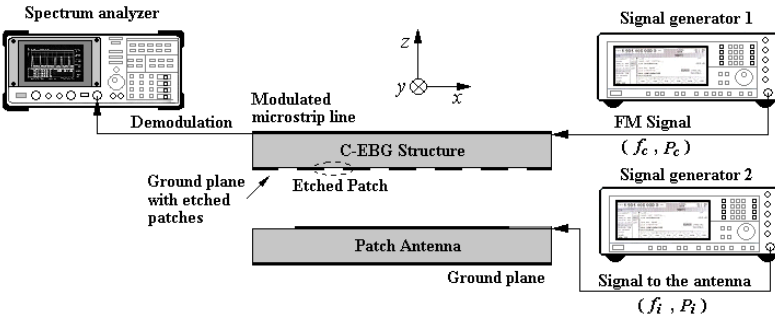


Figure 4. Block diagram of the EMC test setup.

(taken as reference):

$$r_n = \frac{v_{\max} - v_{\min}}{v'_{\max} - v'_{\min}} \tag{3}$$

where  $(v_{\max} - v_{\min})$  is the measured noise P-P voltage when the DUT is exposed to an interference and  $(v'_{\max} - v'_{\min})$  is the measured noise P-P voltage when the DUT is not exposed to an interference.  $r_n$  is used to evaluate the increase in the noise P-P voltage on the transmitted signal in the DUT when it is subjected to an interference caused by nearby radiation. A high  $r_n$  implies large increase in noise level due to the interference. The additional noise is considered to be insignificant when  $r_n = 1$ .  $r_n$  indicates the level of interference suffered by the DUT in an EM environment rich in radiation.

Before subjecting the structure to interference, the FM signal with a carrier frequency ranging from 1 GHz to 4 GHz at step intervals of 0.5 GHz are transmitted through the DUT. The noise P-P voltages without any interference and only due to the structure itself (ripple level) are recorded and the normalized values are plotted in Fig. 5. For the purpose of comparison, the normalized measured  $|S_{21}|$  of the DUT is also plotted in Fig. 5. As can be seen in Fig. 5, the normalized  $|S_{21}|$  has the same trend as that of the normalized  $(v'_{\max} - v'_{\min})$  over the entire passband, which indicates the effect of ripples of the DUT on its noise P-P value. When the ripple level is high, the noise P-P voltage is correspondingly high and vice versa. In order to take into account the effect of ripple for the EMS experiment, this measured noise P-P voltage,  $(v'_{\max} - v'_{\min})$ , is used as reference.

With the experimental setup introduced above, by using the relative noise P-P voltage as a parameter for the evaluation of EMS

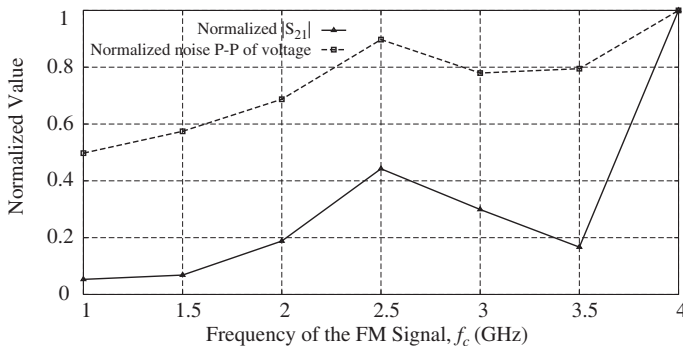


**Figure 5.** The normalized simulated  $|S_{21}|$  and the normalized noise P-P voltage of the signal transmitted through the C-EBG filter structure.

of the structure, the effect of the interference source and those of the relative position or polarization between the DUT and the radiating interference source are investigated and presented in Sections 3.2 and 3.3, respectively.

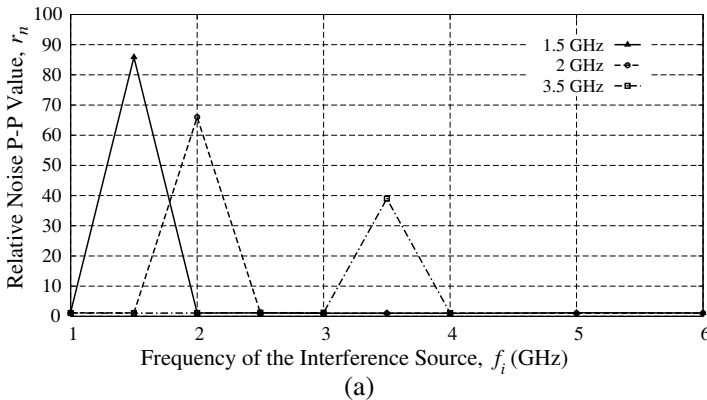
### 3.2. Frequency and Power Level of the Radiating Interference Source

In order to study the effect of the interference source at various working frequencies and power levels, parameters that determine the relative position (or polarization) between the radiating interference source and the DUT such as  $\theta$  and  $d$  (or  $\phi$ ) are fixed.  $\theta = \pm 90^\circ$  (MLIN plane or GND plane),  $\phi = 0^\circ$ , and  $d$  is set in such a way that the DUT is in the near-field or far-field region of the interference source.

#### 3.2.1. Frequency, $f_i$

An FM signal with a power level  $P_c = -30$  dBm and carrier frequency  $f_c = 1.5$  GHz, 2 GHz, and 3.5 GHz are transmitted through the DUT respectively. The frequency of the interference source ( $d = R_1$ ,  $\theta = \pm 90^\circ$  (towards the MLIN plane or GND plane),  $\phi = 0^\circ$ )  $f_i$  is varied from 1 GHz to 7 GHz and the power level is fixed at  $-15$  dBm ( $P_i = -15$  dBm). The noise P-P voltages of the demodulated FM signal are recorded and the relative noise P-P voltages are calculated using (3) and plotted in Fig. 6.

Figures 6(a) and (b) show the relative noise P-P voltage of the FM signal with a fixed  $f_c$  ( $f_c = 1.5$  GHz, 2 GHz, 3.5 GHz) when  $\theta = 90^\circ$  and  $-90^\circ$ , respectively. From Fig. 6(a), it can be seen that at  $\theta = 90^\circ$  where the MLIN plane is exposed to the interference source, the signal in the





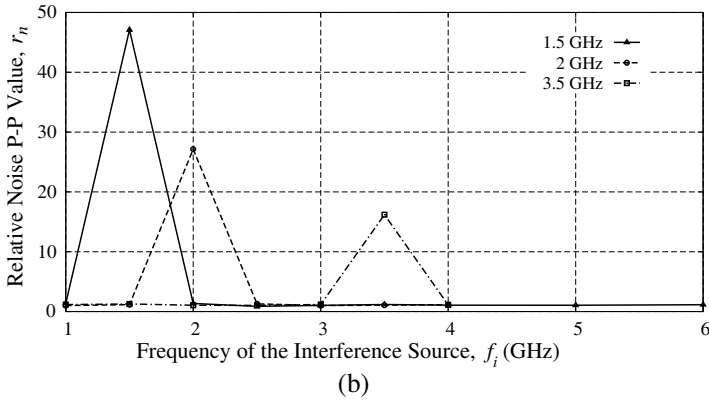


**Figure 6.** The relative noise P-P voltage of the demodulated FM signal ( $f_c = 1.5$  GHz, 2 GHz, 3.5 GHz) at the output of the C-EBG filter when the frequency of the interference source,  $f_i$ , is varied from 1 GHz to 7 GHz. (a) Towards MLIN plane. (b) Towards GND plane.

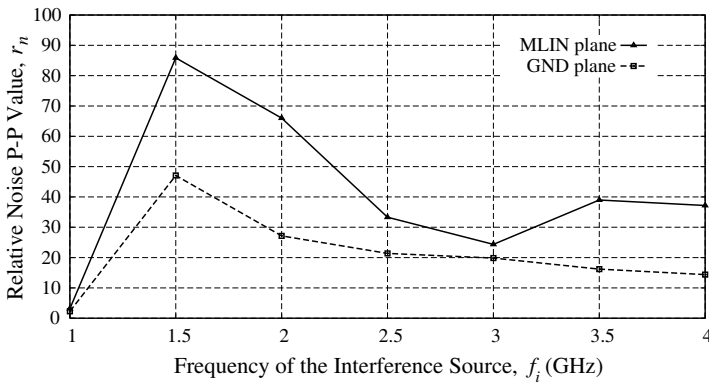


**Figure 7.** The relative noise P-P voltage of a demodulated FM signal at the output of the C-EBG filter when  $f_i = f_c$ .

DUT at 1.5 GHz, 2 GHz, and 3.5 GHz has a maximum relative noise P-P value ( $r_{n-max}$ ) of 85.87, 66.00, and 39.00 when the working frequency of the interference source is the same as that of the signal transmitted through the DUT. Similarly the interference level is the highest when both working frequencies are the same. This is expected since when the frequency of the interferer is the same as the working carrier frequency, it will cause the most interference and thus the interference level will be the highest.

At the maximum points when  $f_i = f_c$ , a further study is conducted

with  $f_i = f_c$ . A frequency sweep over the passband (from 1 GHz to 4 GHz) at frequency steps of 0.5 GHz is performed.  $\theta$  is set to be  $90^\circ$  and  $-90^\circ$ .  $r_n$  of the signal are obtained and plotted in Fig. 7. As can be seen in Fig. 7,  $r_n$  varies a lot when the frequency is varied. In both cases, the noise level of the signal with  $f_i = f_c$  is frequency dependent. When the MLIN plane is exposed to the interference source,  $r_n$  has the maximum value of 85.87 at  $f_i = f_c = 1.5$  GHz and a minimum value of 3.18 at  $f_i = f_c = 1$  GHz among all the frequencies. When the GND plane is exposed to the interference source, the curve also has a maximum value of 47.08 at 1.5 GHz and a minimum value of 2.27 at 1 GHz.

The results obtained reveal that the susceptibility of the C-EBG filter structure to the interference is frequency dependent. This particular structure has good immunity at 1 GHz even with an interference source placed in close proximity and working at the same frequency as the frequency of the signal in the structure. However, the susceptibility of the structure is considerably high at 1.5 GHz when it is working at the same frequency as that of the interference source.

In Fig. 7, it also shows that  $r_n$  is dependent on the relative position of the interference source with respect to the DUT,  $\theta$ . It is observed that  $r_n$  is consistently higher when the MLIN plane is exposed to the interference source than that when the GND plane is exposed to the interference source. This indicates better immunity of the defected ground plane of the C-EBG filter structure as compared to that of the modulated MLIN. As a result of the observation, for the ease and accuracy of observation,  $f_i$  and  $f_c$  are both set to be 1.5 GHz in the following experiments due to the high susceptibility of the DUT at this frequency.

In addition, a comparison is made between Fig. 5 and Fig. 7. It is observed that although the ripple level or noise figure of the C-EBG filter structure is the highest at 4 GHz (Fig. 5), this does not necessarily suggest a poor susceptibility of the structure at the same frequency (Fig. 7). In fact, from Fig. 7, the susceptibility of the C-EBG filter is relatively good at 4 GHz as compared to 1.5 GHz.

**Guideline 1:** *The working frequency or the harmonics of a nearby radiating circuit component should be different from the working frequency of a C-EBG microstrip filter structure.*

### 3.2.2. Power, $P_i$

In the experiment,  $\theta = 90^\circ$ ,  $\phi = 0^\circ$ , and the interference source is placed  $d = [R_1 + 0.5(R_1 - R_2)]$  and  $d = 1.2R_2$  away from the DUT for the near-field and far-field test, respectively. An FM signal ( $f_c = 1.5$  GHz,  $P_c = -30$  dBm) is transmitted through the DUT. In order to

obtain a strong interference for easy detection and measurement, both  $f_i = f_c = 1.5$  GHz. The noise P-P values of the FM signal transmitted through the DUT are recorded at the output of the device when the power level of the interference source,  $P_i$ , is varied from  $-15$  dBm to  $-45$  dBm. The relative noise P-P values are calculated and plotted in Fig. 8.

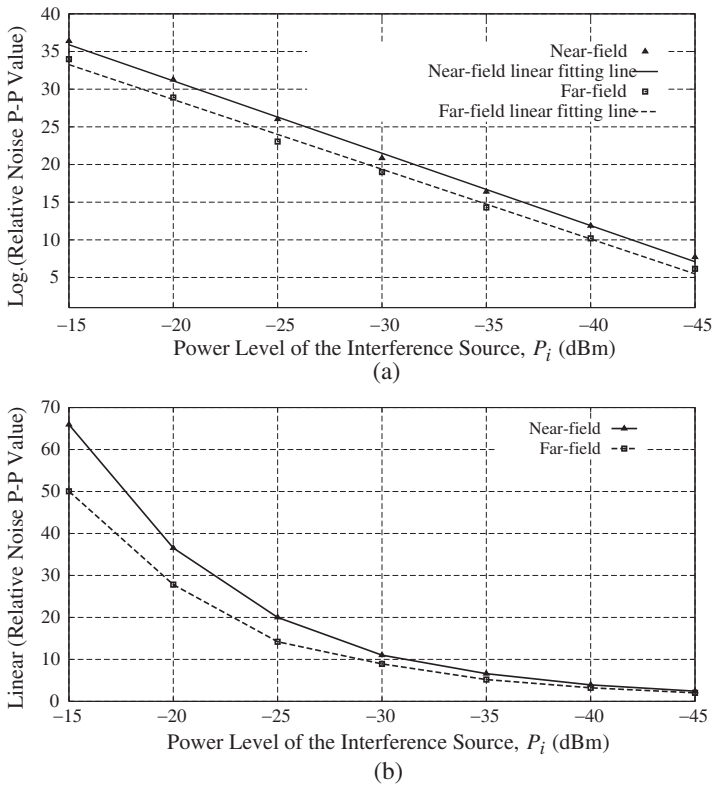


**Figure 8.** The relative noise P-P voltage of a demodulated FM signal at the output of the C-EBG filter when the power of the interference source,  $P_i$ , is varied from  $-15$  dBm to  $-45$  dBm. (a) Log-Log. scale. (b) Linear-Log. scale.

Figures 8(a) and (b) show the logarithm and the real value of  $r_n$ , respectively. As can be seen in Fig. 8(a), in both the near- and far-field region, the logarithm of  $r_n$  decreases linearly as the power level of the interference source decreases, which is expected since the power level of the interference source has a linear relationship with logarithm of the noise level. In Fig. 8(b), a knee is observed when  $P_i = -30$  dBm where  $r_n$  drops below 15.00 in both the near- and far-field region.

This indicates that the C-EBG filter is relatively unsusceptible to the interference when the power of the interference source equals or lower than that of the signal transmitted through the DUT.

**Guideline 2:** *If a radiating interference source is working at the same frequency as that of a C-EBG structure, its power level should be reduced to be equal or less than that of the C-EBG structure.*

### 3.3. Relative Position and Polarization of the Radiating Interference Source

From the results obtained above, the effects of either the frequency or the power level of a radiating interference source on the signal transmission through the C-EBG filter structure are significant. However, in some applications, the working frequency and the power level of a nearby radiating circuit component can not be modified to eliminate the interference to the EBG structure. In such circumstances, the knowledge on the effect of the relative position and polarization of the radiating interference source with respect to the DUT would be useful for minimizing interference. In this part of the paper, the distance between the DUT and the interference source  $d$ , the angle of incidence of the radiating interference source to the DUT  $\theta$ , and the polarization  $\phi$  are examined. Again,  $f_c = f_i = 1.5$  GHz to obtain a high interference level. The power of the transmitted signal through the DUT is set to be  $-30$  dBm and the power level of the interference source is set to be  $-15$  dBm.

#### 3.3.1. Relative Distance, $d$

At  $f_i = 1.5$  GHz,  $R_1$  (inner boundary) and  $R_2$  (outer boundary) of the radiating near-field region of a patch antenna are determined to be 43.22 mm and 98.12 mm according to (1) and (2), respectively.  $d$  is varied from  $R_1$  to  $1.5R_2$  with  $\phi = 0^\circ$  and  $\theta = +90^\circ$  (MLIN) or  $-90^\circ$  (GND).

Figure 9 plots the recorded relative noise P-P value of the signal transmitted through the DUT when the interference source is directed towards the MLIN plane ( $\theta = +90^\circ$ ) or towards the GND plane ( $\theta = -90^\circ$ ). As shown in Fig. 9, when the MLIN plane is subjected to the interference,  $r_n$  decreases as  $d$  increases. This is expected since the strength of the  $E$ -field of the interference source decreases as  $d$  increases. In the near-field region, the rate of decrease in  $r_n$  is high decreases when  $d$  increases from 43.22 mm to 98.12 mm.  $r_n$  becomes relatively small when  $d > 81.65$  mm ( $0.41\lambda$ ). In the far-field region,  $r_n$  decreases linearly when  $d$  is increased. When the GND plane is exposed to the interference source, as can be seen in Fig. 9, the noise

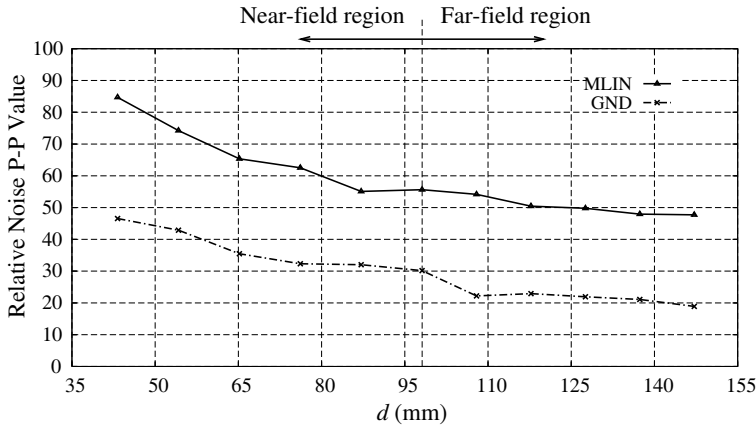


**Figure 9.** The relative noise P-P voltage of a demodulated FM signal at the output of the C-EBG filter when the distance,  $d$ , is varied from near-field to far-field region.

level of the signal decreases in a similar manner to that when the MLIN plane is subjected to the interference source. It is also found that the linear relationship between  $r_n$  and  $d$  in the far-field is the same for both cases, regardless of the plane that is subjected to the interference source. The noise level of the signal through the C-EBG filter is relatively predictable when it is placed in the far-field region as compared to the near-field region. The structure is less susceptible to the interference when it is placed  $0.41\lambda$  away from the interference source. In Fig. 9, it is again found that the noise level of the signal is much lower when the GND plane is subjected to the interference than that when the MLIN plane is subjected to the interference. The effect of  $\theta$  will be studied in detail in the next section.

**Guideline 3:** A C-EBG structure should be placed in the far-field region of the radiating interference source in order to avoid severe interference.

### 3.3.2. Angle of Incident, $\theta$

As has been shown in Fig. 7 and Fig. 9, the FM signal transmitted through the DUT has higher  $r_n$  when the MLIN plane is exposed to the interference source ( $\theta = +90^\circ$ ) as compared to that when the GND is exposed to the interference source ( $\theta = -90^\circ$ ). From this results, it can be deduced that  $\theta$  has a considerable effect on the amount of interference on the DUT. The difference is dependent on the working

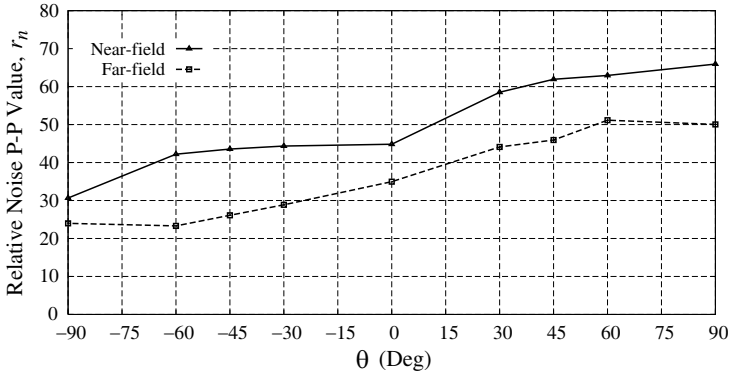


**Figure 10.** The relative noise P-P voltage of a demodulated FM signal at the output of the C-EBG filter when the angle of incidence of the radiating interference source to the DUT  $\theta$  is varied from  $-90^\circ$  to  $+90^\circ$ .

frequency when  $f_c = f_i$  as can be seen in Fig. 7. It has a small variation when the distance between the interference source and the DUT is varied, which can be seen in Fig. 9. The effect of  $\theta$  is further examined in this section. With  $f_i = f_c = 1.5$  GHz, the interference source is placed 70.67 mm and 117.74 mm away from the C-EBG filter for the near-field and far-field test, respectively.  $\phi$  is set to  $0^\circ$  and  $\theta$  is varied from  $-90^\circ$  to  $90^\circ$ .

The noise levels of the signals under test are measured and plotted in Fig. 10. As seen in Fig. 10, in both the near-field and the far-field region,  $r_n$  increases as  $\theta$  increases from  $-90^\circ$  to  $+90^\circ$ . The interference level that the signal suffers is higher when  $\theta > 0^\circ$  than that when  $\theta < 0^\circ$ . This implies that the MLIN of the DUT is more susceptible to the interference than the GND. The reason is that when the MLIN plane is exposed to the interference source, the  $E$ -field of the antenna directly interferes the signal transmitted through the C-EBG filter structure while when the GND is exposed to the interference source, the interference can only get through to the signal line through the etched circles in the ground plane. As can be seen in Fig. 10, the DUT has a  $r_n$  larger than 20 when the radiating interference source is directed to the GND. It is additional interference suffered by the DUT as compared to the one with a perfect GND which is introduced by the etched circular patches in the GND.

**Guideline 4:** In a multi-layer circuit, a radiating component is suggested to be placed under the GND of a C-EBG structure in order to eliminate interference.

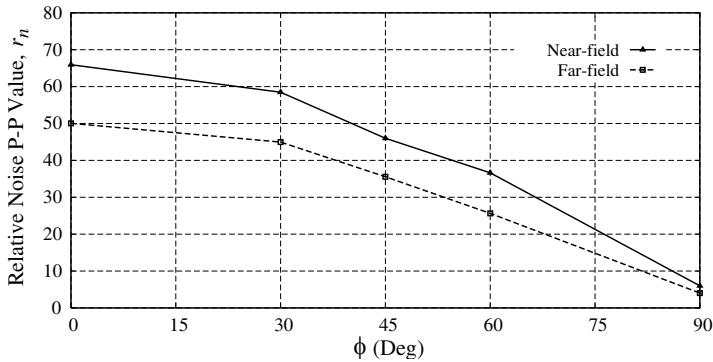


**Figure 11.** The relative noise P-P voltage of a demodulated FM signal at the output of the C-EBG filter when the angle of polarization,  $\phi$ , is varied from  $0^\circ$  to  $90^\circ$ .

### 3.3.3. Polarization, $\phi$

The study on the effect of the polarization of the interference source  $\phi$  is conducted in both the near-field ( $d = 70.67$  mm) and the far-field region ( $d = 117.74$  mm).  $\phi$  is varied from  $0^\circ$  to  $90^\circ$  and  $\theta$  is set to be  $90^\circ$  and  $-90^\circ$ .

Figure 11(a) shows the calculated relative noise P-P values of the measured demodulated FM signals. As shown in Fig. 11,  $r_n$  of the signal decreases dramatically as  $\phi$  increases from  $0^\circ$  to  $90^\circ$  in both near-field and far-field region.  $r_n$  decreases at an increasing speed when  $\phi > 30^\circ$ . The signal has an  $r_n$  of 6.00 and 4.03 at  $\phi = 90^\circ$  in the near-field and far-field region, respectively, which are close to 1. It indicates that the interference is negligible at  $\phi = 90^\circ$  where the polarization of the  $E$ -field of the interference source is perpendicular to the direction of the signal transmission and a minimum cross polarization interference is obtained.

**Guideline 5:** A relative cross polarization is suggested for a low interference level introduced by a radiating interference source to a C-EBG structure.

In this part of the study, the EMS of a dual-plane C-EBG microstrip structure to a radiating interference source has been studied. The effects of the frequency and power of the interference source are severe. The interference level is the highest in all when the frequency of the signal transmitted in the DUT equals that of the interference source. The amount of interference decreases linearly as the power level of the interference source decreases.

The relative position and polarization between the DUT and the

interference source also have significant effects on the interference to the DUT. The interference level that the signal in the DUT suffers decreases when the distance between the two structures increases. It becomes small at an acceptable level when the interference source is placed at least  $0.41\lambda$  away from the DUT. A low interference level can also be obtained by changing  $\theta$  or  $\phi$ . Although the GND with etched patches causes additional interference to the DUT as compared to a microstrip structure with perfect GND, it has better immunity to interference as compared to the MLIN plane. When  $\phi = 90^\circ$ , the interference is negligible because the polarization of the  $E$ -field of the interference source is perpendicular to the direction of the signal transmission in the DUT.

#### 4. INTERFERENCE CAUSED BY A COPLANAR MLIN

The second part of the EMS study involves an interference introduced by the disturbance or coupling of a MLIN that is placed close to the DUT and on the same plane as that of the structure (coplanar MLIN). Two types of EM influence caused by the coplanar MLIN to the DUT are studied. Case one is the influence of a passive coplanar MLIN on the  $S$ -parameters of the C-EBG filter structure when no signal is transmitting through the coplanar MLIN and it is at close proximity. Case Two is the effect of coupling caused by the signal transmitted through the coplanar MLIN to the performance of the DUT.

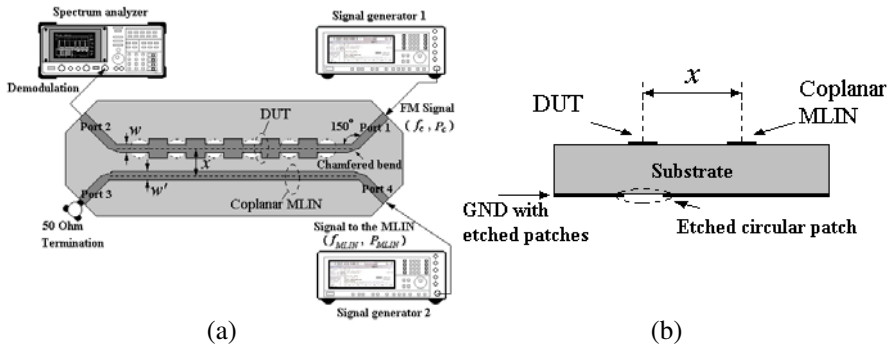


**Figure 12.** The structure under EMC testing. (a) Top view. (b) Cross sectional view.



#### 4.1. Experimental Setup

Figures 12(a) and (b) show the top view and cross sectional view of the DUT with a coplanar MLIN, respectively. The block diagram of the experimental setup for the testing in Case Two is incorporated in Fig. 12(a). As shown in Fig. 12(a), a coplanar MLIN with a width of  $w'$  is placed  $x$  away from the C-EBG structure in the transversal direction on the plane where the MLIN with inserted patches of the C-EBG structure is located. Both MLIN's are bent at an angle of  $150^\circ$  at the input and output ports to ease testing when  $x$  is small. The bends are chamfered at a chamfering percentage [11] of 5% to compensate additional loss introduced by the bend. The port numbers are also shown in Fig. 12(a). As can be seen in Fig. 12(b), the interference source is on the same plane as that of the C-EBG structure under test.

#### 4.2. Case One: Influence of a Passive Coplanar MLIN

The DUT with a coplanar MLIN  $x$  away from it are simulated using *Zeland IE3D<sup>TM</sup>*.  $x$  is set to 4.5 mm, 6.5 mm, 8.5 mm, 10.38 mm, 15 mm, and 20.76 mm where 10.38 mm is exactly one period of the structure  $a$  and  $20.76 \text{ mm} = 2a$ . In the simulation, there is no signal going through the MLIN. Fig. 13 shows the simulated  $S_{21}$ -parameters of the DUT with a passive coplanar MLIN  $x$  away from it (where  $x = 4.5 \text{ mm}$ ,  $6.5 \text{ mm}$ ,  $8.5 \text{ mm}$ , and  $a$ ). The simulated data of the DUT itself are also included in Fig. 13 for the purpose of comparison. As

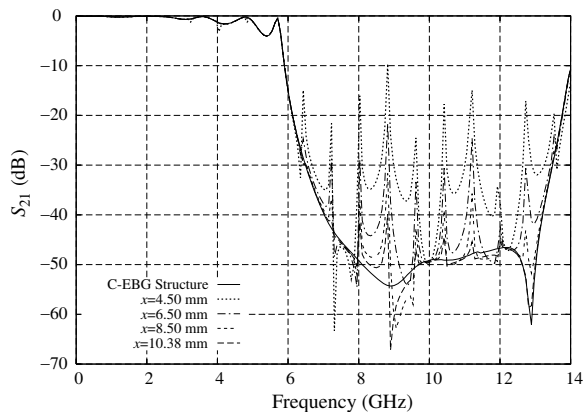
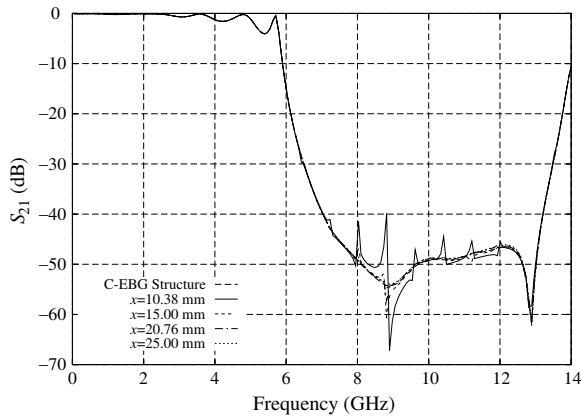


**Figure 13.** The simulated  $S_{21}$ -parameter of the C-EBG filter structure and those of the structures with a coplanar MLIN ( $x = 4.5 \text{ mm}$ ,  $6.5 \text{ mm}$ ,  $8.5 \text{ mm}$ , and  $a$ ).

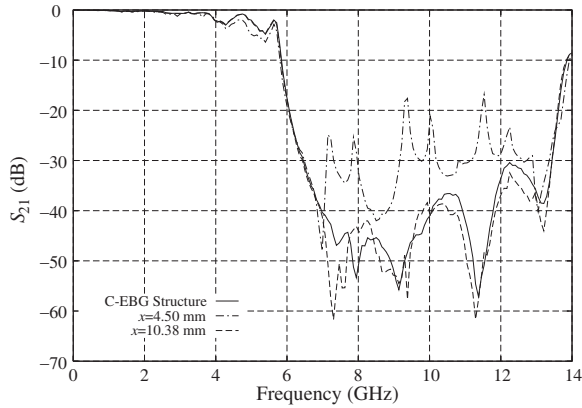
can be seen in Fig. 13, each DUT shows a stopband over the same frequency range, which indicates that the passive coplanar MLIN does not affect the center frequency of the stopband of the DUT. However, the smoothness of the stopband is severely affected. The DUT with an  $x$  of 4.5 mm, 6.5 mm, 8.5 mm, and 10.38 mm ( $a$ ) shows a maximum ripple level of  $-9.64$  dB,  $-21.67$  dB,  $-31.69$  dB, and  $-40.00$  dB in the stopband, respectively. Furthermore, additional ripples are observed in the passband of the DUT with a MLIN 4.5 mm away from it. No additional ripples are found in the passbands of the other three C-EBG structures.

Figure 14 shows the simulated  $S_{21}$ -parameters of the DUT with a coplanar MLIN farther away from it than those structures in Fig. 13 ( $x = a$ , 15 mm,  $2a$ , and 25 mm). Again, the simulated transmission coefficient of the DUT itself is also included. As shown in Fig. 14, no decrease in attenuation or large ripples in the stopband are found when  $x$  is varied beyond one period of the structure. There is no increase in the ripple level in the passband while the ripple level in the stopband vanishes when  $x$  increases to 25 mm. As can be seen in Fig. 14, with  $x \geq a$ , the effect of a passive coplanar MLIN is negligible and the performance of the DUT is not affected.

The C-EBG filter structure with a coplanar MLIN 4.5 mm and  $a$  away from it are fabricated to verify the simulation results. Fig. 15 shows the measured  $S$ -parameters of the DUT with a coplanar MLIN 4.5 mm and 10.38 mm away from it. The measured  $S_{21}$ -parameter of



**Figure 14.** The simulated  $S_{21}$ -parameter of the C-EBG filter structure and those of the structures with a coplanar MLIN ( $x = a$ , 15 mm,  $2a$ , and 25 mm).



**Figure 15.** The measured  $S_{21}$ -parameters of the fabricated C-EBG filter structures with and without a coplanar nearby MLIN.

the DUT itself is also included in Fig. 15 for the purpose of comparison. As can be seen from Fig. 15, the DUT with an  $x$  of 4.5 mm shows a maximum ripple level of  $-17.60$  dB in the stopband and a ripple level of  $6.42$  dB in the passband whereas the structure with an  $x$  of 10.38 mm shows a similar frequency response to that of the DUT itself. No additional ripple in the stopband or passband is observed. The measured results are in good agreement with the simulated results.

The results obtained reveal that a nearby coplanar MLIN without signal significantly affects the  $S$ -parameters of the C-EBG structure in terms of ripple level in both the passband and the stopband when  $x$  is small, e.g.,  $x = 4.5$  mm. The increase in ripple level is due to the disturbance introduced by the coplanar MLIN nearby through the shared substrate. The ripple level decreases significantly as  $x$  increases, which is due to the high confinement of electromagnetic fields around the MLIN. If material with a higher  $\epsilon_r$  is used as compared to Taconic,  $x$  can be smaller with no interference. The ripple level becomes acceptable when  $x \geq a$ .

The influence of a passive coplanar MLIN on the frequency response of the DUT depends on the distance between the two microstrip structures. Since a high ripple level in the stopband degrades the performance of the filter, the distance between the DUT and the coplanar MLIN has a minimum value,  $x_{\min}$ , where the EM influence of the coplanar MLIN is at an acceptable level.

**Guideline 6:** *When integrating a C-EBG structure into MMICs, the nearest coplanar MLIN should be at least one period away from the structure in order to have small electromagnetic effect when the coplanar MLIN stands idle.*

### 4.3. Case Two: Effect of Coupling of a Coplanar MLIN with a Signal

When a signal is transmitted through the coplanar MLIN, coupling is introduced through the share substrate to the DUT that affects its performance. The experimental setup is illustrated by the block diagram in Fig. 12(a). As shown in Fig. 12(a), similar to the study on the EMS of the DUT to a nearby radiating interference source in the last section, an FM signal with a carrier frequency  $f_c$  is transmitted through the DUT while a PW signal at a frequency  $f_{MLIN}$  is transmitted through the coplanar MLIN. The DUT is exposed to the coupling introduced by the coplanar MLIN that is transmitting a signal. The FM signal is recorded and demodulated at the output of the DUT. The relative noise P-P voltage defined using (3) is calculated and used to evaluate the EMS characteristics of the DUT.

The coplanar MLIN is placed sufficiently far ( $x > x_{\min}$ ) to avoid EM influence according to the previous study. The dual-plane C-EBG structure with a coplanar MLIN 10.38 mm, 15 mm, 20.76 mm, and 25 mm away from it are tested.

#### 4.3.1. Frequency of the Interference Source, $f_{MLIN}$

An FM signal with a power level of  $-30$  dBm and a carrier frequency of 1 GHz and 4 GHz are respectively transmitted through the C-EBG microstrip filter structure. The DUT is exposed to the interference whose frequency is swept from 1 GHz to 7 GHz with a fixed power level of  $-20$  dBm. The noise P-P voltages of the demodulated FM signal are recorded when the DUT is exposed to the interference at different frequencies and the relative noise P-P voltages are calculated using (3) and plotted.

Figures 16(a) and (b) show the relative noise P-P voltage of the FM signals ( $f_c = 1.5$  GHz, 2.5 GHz, 3.5 GHz) with the coplanar MLIN  $a$  and 15 mm away from the DUT, respectively. As shown in Fig. 16(a),  $r_n$  of the FM signal with a  $f_c = 1.5$  GHz has a maximum value at 1.5 GHz. Similarly, the FM signal with a  $f_c = 2.5$  GHz and a  $f_c = 3.5$  GHz, respectively, has a maximum  $r_n$  at 2.5 GHz and 2.5 GHz. In Fig 16(b), the peak value of the relative noise P-P voltage is also found at the  $f_{MLIN}$  when  $f_{MLIN} = f_c$ . Peak values are found when the coplanar MLIN and the DUT are operating at the same frequency. The noise level sinks when the coplanar MLIN is further away.

The results above again reveal that the interference level is the highest when the interference frequency is the same as the carrier frequency. In both Figs. 16(a) and (b), it can also be seen that when  $f_{MLIN} = f_c$ , as the frequency increases, the peak interference level

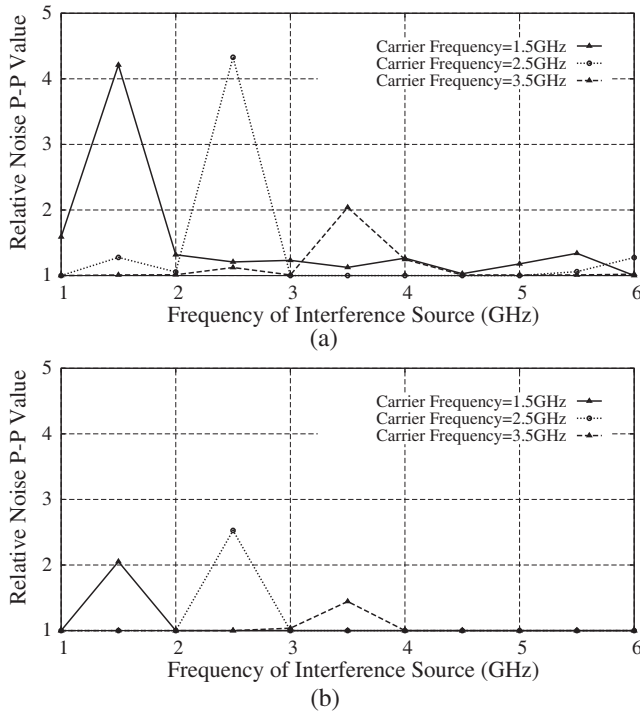


**Figure 16.** The measured relative noise peak-peak voltage of the demodulated FM signal ( $f_c = 1.5$  GHz, 2.5 GHz, 3.5 GHz, power level =  $-30$  dBm) when the frequency of the interference source is varied (power level =  $-20$  dBm). (a)  $x = a$ . (b)  $x = 15$  mm.

decreases considerably. This is because when the frequency increases from 1.5 GHz to 3.5 GHz,  $a$  varies from  $0.075\lambda_g$  to  $0.175\lambda_g$ , which is equivalent to an increase in the distance between the two microstrip structures. An exception is found at  $f_c = 2.5$  GHz, which is probably due to other external interference sources. Additionally, the results also reveal that a small  $x$  results in a high interference level. The relation between  $x$  and the level of interference is to be discussed in details in Section 3.

To obtain a high interference level,  $f_{MLIN}$  is set to equal to  $f_c$  in the following experiments for ease of observation.

**Guideline 7:** The frequencies of the signals transmitted through a coplanar MLIN and a C-EBG structure that are at close proximity should avoid to be the same in order to avoid high interference introduced by the coplanar MLIN to the C-EBG structure. It is consistent with Guideline 1.

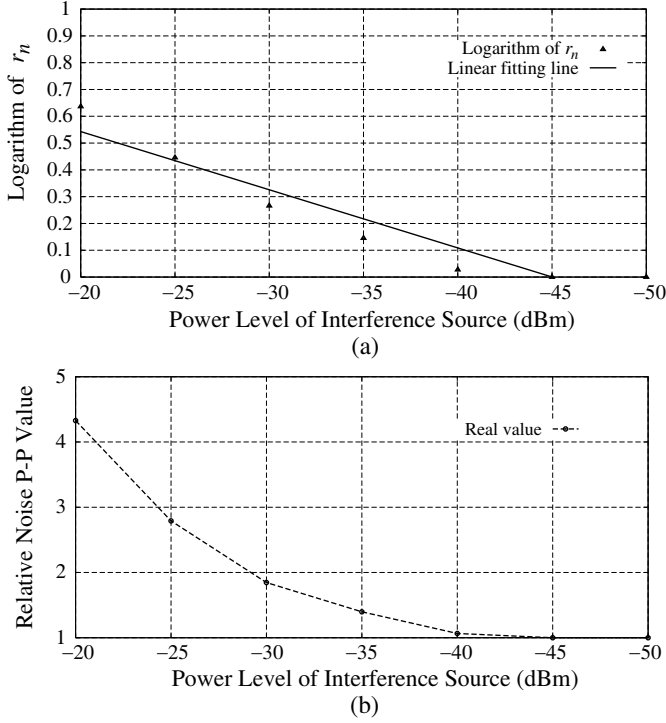


**Figure 17.** The measured relative noise peak-peak voltage and the linear fitting line of the demodulated FM signal (power level of the signal in the C-EBG structure =  $-30$  dBm,  $x = 10.38$  mm) when the power level of the interference source is varied. (a) Logarithm. (b) Real value.

#### 4.3.2. Power Level of the Interference Source $P_{MLIN}$

An FM signal (power level =  $-30$  dBm; carrier frequency =  $1.5$  GHz) is transmitted through the DUT. The power level of the interference is varied from  $-20$  dBm to  $-50$  dBm and  $f_{MLIN} = f_c$ . The noise P-P voltages are recorded at each power level of the interference and the relative noise P-P voltages are calculated and plotted.

Figures 17(a) and (b) show the logarithm and the real value relative noise P-P voltages of the C-EBG filter structure with an  $x = a$  at a carrier frequency of  $1.5$  GHz. The logarithm of  $r_n$  decreases linearly as the power level of the interference source decrease, which is as expected and is similar to that observed in the study where a radiating interference source is involved. As shown in Fig. 17(b), the

real value of  $r_n$  decreases at a decreasing rate and the rate of decrease falls at around  $P_{MLIN} = -30$  dBm that is the same as the power level of the signal in the DUT.

**Guideline 8:** *If a coplanar MLIN and a C-EBG structure are working at the same frequency, the power level of a signal through a nearby coplanar MLIN should be equal or lower than that of the signal through the C-EBG structure. It is consistent with Guideline 2.*

#### 4.3.3. Distance, $x$

As presented, the C-EBG filter structure under test is susceptible to the variation of the frequency or power level of the interference caused by the nearby coplanar MLIN with a transmitted signal. The results above also indicate the effect of the distance between the two microstrip structure on the performance of the DUT.

The power level of the signal in the DUT is set to be  $-30$  dBm and that of the signal in the coplanar MLIN is set to be  $-20$  dBm. With  $f_{MLIN} = f_c$ , the signal in the DUT is tested and the relative noise P-P voltages are calculated and plotted.

Figure 18 shows the relative noise P-P voltages of the FM signal transmitted in the DUT at a  $f_c$  (where  $f_c = 1.5$  GHz, 2.5 GHz, and 3.5 GHz). As can be seen in Fig. 18,  $r_n$  decreases with an increase in the distance between the two microstrip structures in each case. It is also observed that the rate of decrease in  $r_n$  is high when  $x$  is over the range of 10 mm to approximately 15 mm and the decrease slows down when  $x$  goes beyond 15 mm. There is a knee at around  $x = 15$  mm.

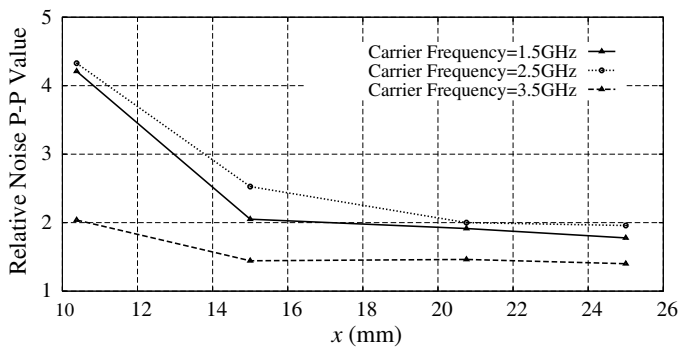


**Figure 18.** The measured relative noise peak-peak voltage of the demodulated FM signal (power level of the signal in the C-EBG structure =  $-30$  dBm, power level of the interference source =  $-20$  dBm) when  $x$  is varied.

The knee is mainly due to the high confinement of electromagnetic fields around the MLIN. It is also observed that, at each  $x$  under test, the interference level is much lower when the working frequency is high (e.g., 3.5 GHz) as compared to those when the frequency is relatively low. This is because an electrical distance of the two structure increases as the working frequency increases. Again, an exception is observed at 2.5 GHz which is probably due to external interference source.

**Guideline 9:** *A coplanar MLIN should be placed far enough away from a C-EBG structure in order to eliminate the effect of coupling caused by the signal transmitted through the coplanar MLIN on the performance of the C-EBG structure. A knee should be identified where a relative small distance and low interference level can be obtained simultaneously. A small distance is allowed at high working frequencies.*

## 5. CONCLUSION

This paper presents a detailed study on the susceptibility of a dual-plane compact EBG microstrip filter structure to interference that it may encounter when it is integrated to a circuit board with other components. The EMS of the DUT is investigated under two scenarios with high possibility: one has a radiating interference source and the other has a coplanar MLIN in a close proximity.

The susceptibility to a nearby radiation is examined through experimental results. The frequency and power level of the interference source as well as the relative position and polarization of the interference with respect to the DUT are four key factors that significantly affect the performance of the DUT.

The EM effects on the C-EBG structure due to a nearby coplanar MLIN with and without a signal are both included, respectively. The distance between the two structures affects the performance of the DUT regardless the existence of the signal in the nearby coplanar MLIN. When there is a signal transmitted in the coplanar MLIN, similar to the effect of a nearby radiation, the frequency and power level of the signal are crucial factors that affect the response of the DUT.

Base on the results obtained, guidelines for the applications of a C-EBG structure are summarized as followed:

- (i) C-EBG structure and a nearby circuit component should have different working frequencies.
- (ii) If a C-EBG structure has to have the same working frequency as that of a nearby circuit component, the power level of the nearby



component should be equal to or less than that of the C-EBG structure.

- (iii) If the working frequency and power level of both structures are fixed and the interference level of a C-EBG structure is high, the C-EBG structure should be kept far away from the interference source to lower the interference level. For a radiating interference source, alternatively, the C-EBG structure is suggested to direct the GND towards the interference source or/and orientate to obtain a cross polarization, in order to lower interference level.
- (iv) For interference caused by a coplanar MLIN, the C-EBG structure should be kept one period away from the coplanar MLIN so as to eliminate the EM effect of a passive coplanar MLIN.

## REFERENCES

1. Garcia-Garcia, J., J. Bonache, and F. Martin, "Application of electromagnetic bandgaps to the design of ultra-wide bandpass filters with good out-of-band performance," *IEEE Transactions on Microwave Theory and Techniques*, Vol. 54, No. 12, 4136–4140, 2006.
2. Yang, F., K. Ma, Y. Qian, and T. Itoh, "A uniplanar compact photonic-bandgap (UC-PBG) structure and its applications for microwave circuit," *IEEE Transactions on Microwave Theory and Techniques*, Vol. 47, No. 8, 1509–1514, 1999.
3. Falcone, F., T. Lopetegi, and M. Sorolla, "1-D and 2-D photonic bandgap microstrip structures," *Microwave and Optical Technology Letters*, Vol. 22, No. 6, 411–412, 1999.
4. Huang, S. Y. and Y. H. Lee, "Tapered dual-plane compact electromagnetic band-gap microstrip filter structure," *IEEE Transactions on Microwave Theory and Techniques*, Vol. 53, No. 9, 2656–2664, 2005.
5. Akalin, T., M. A. G. Laso, T. Lopetegi, O. Vanbesien, M. Sorolla, and D. Lippens, "PBG-type microstrip filters with one- and two-sided patterns," *Microwave and Optical Technology Letters*, Vol. 30, No. 1, 69–72, 2001.
6. Du, Z., K. Gong, J. S. Fu, B. Gao, and Z. Feng, "Influence of a metallic enclosure on the  $S$ -parameters of microstrip photonic bandgap structures," *IEEE Transactions on Electromagnetic Compatibility*, Vol. 44, No. 2, 324–328, 2002.
7. Lee, Y. H. and S. Y. Huang, "Electromagnetic compactibility of a dual-planar electromagnetic band-gap microstrip filter structure,"

- Proceedings of the 17th International Zurich Symposium on Electromagnetic Compatibility*, Singapore, 2006.
8. Lee, Y. H. and S. Y. Huang, "Microstrip line coupling to a dual-plane electromagnetic band-gap microstrip filter structure," *Proceedings of International Symposium on Electromagnetic Compatibility*, Barcelona, Spain, 2006.
  9. Radisic, V., Y. Qian, R. Coccioli, and T. Itoh, "Novel 2-D photonic bandgap structure for microstrip lines," *IEEE Microwave and Guided Wave Letters*, Vol. 8, No. 2, 69–71, 1998.
  10. Balanis, C. A., *Antenna Theory Analysis and Design*, 32–33, John Wiley & Sons, New York, 1997.
  11. Gupta, K. C., R. Garg, I. Bahl, and P. Bhartia, *Microstrip Lines and Slotlines*, 204–208, Artech House Inc., 1996.